Supplementary Information (SI) for Physical Chemistry Chemical Physics.

Supplementary Information

Identifying the Active Nickel Sites and Hydrogen Species in the Phosphosulfide Overlayer on the Ni_2P hydrotreating catalyst: A DFT-D3 Study.

Alba B. Vidal*[a], José Luis Peña-Mena[a], Rafael Añez[a], David S. Coll[b], Oscar Hurtado-Aular[c], Aníbal Sierraalta[a], Joaquin L. Brito[d,e]

[a] Laboratorio de Química Física y Catálisis Computacional, Centro de Química "Dr. Gabriel Chuchani", Instituto Venezolano de Investigaciones Científicas (IVIC), Apartado 21827, Caracas, Venezuela.

[b] Laboratorio de Físico Química Teórica de Materiales, Centro de Química "Dr. Gabriel Chuchani", Instituto Venezolano de Investigaciones Científicas (IVIC), Apartado 21827, Caracas, Venezuela.

[c] Departamento de Química, Universidad Nacional del Sur (UNS), Av. Alem 1253, 8000, Bahía Blanca, Argentina.

[d] Laboratorio de Físico Química de Superficies, Centro de Química "Dr. Gabriel Chuchani", Instituto Venezolano de Investigaciones Científicas (IVIC), Apartado 21827, Caracas, Venezuela.

[e] Biomass to Resources Group, Universidad Regional Amazónica IKIAM, Tena, Ecuador.

S1. Surface models

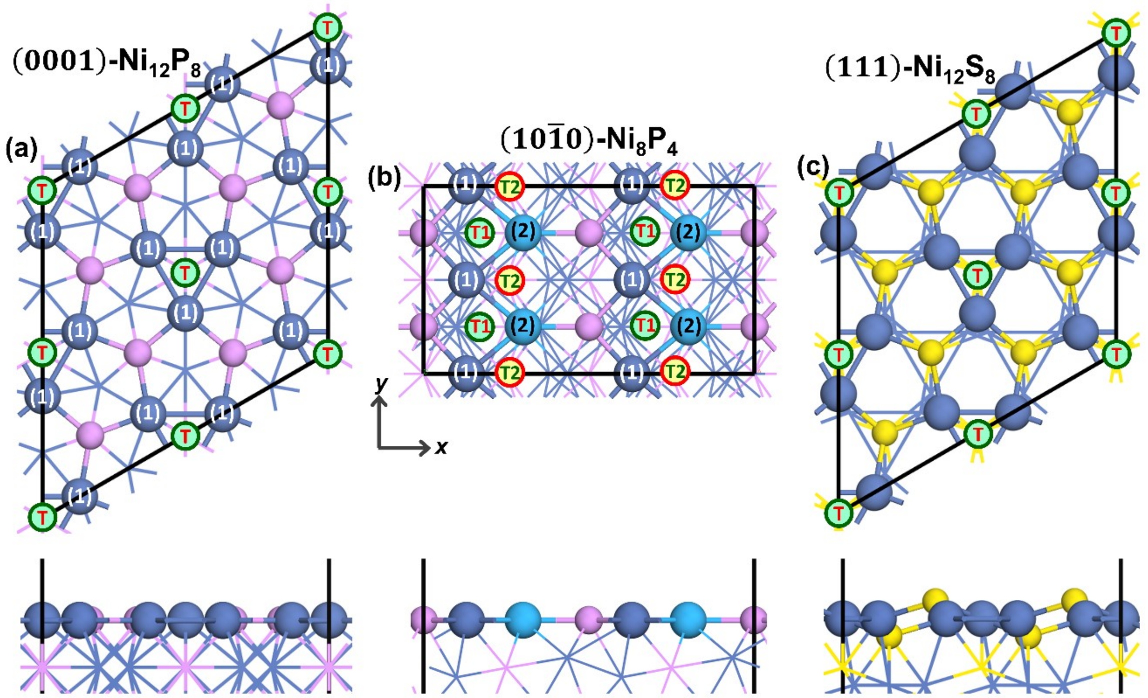

Figure S1. Top and side view of the (2x2) supercell of: (a) (0001) surface and (b) $(10\bar{1}0)$ surface of Ni_2P, and (c) (111) surface of Ni_3S_2. Red and green circles represent the Ni_3 sites present on these surfaces. Blue, pink, and yellow spheres are the nickel, phosphorus, and sulfur atoms, respectively. In the $(10\bar{1}0)$ surface the Ni(2) atoms are represented by light blue spheres.

S2. $\mu_P(T,p)$ and $\mu_S(T,p)$ calculations

The chemical potential of phosphorus, $\mu_P(T,p)$, is determined by the chemical equilibrium with the gas-phase mixture of PH_3 and H_2,

$$\mu_P(T,p) = \mu_{PH_3}(T,p) - \left({}^{3}\!/_{2}\right)\mu_{H_2}(T,p) \tag{S1}$$

$\mu_{PH_3}(T,p)$ and $\mu_{H_2}(T,p)$ are the chemical potentials of PH_3 and H_2, respectively, evaluated assuming ideal gas behavior.

$$\mu_{PH_3}(T,p) = \left[E^{mol}_{PH_3} + \tilde{\mu}_{PH_3}(T,p^0) + RTln\left(\frac{p_{PH_3}}{p^0}\right)\right] \tag{S2}$$

$$\mu_{H_2}(T,p) = \left[E^{mol}_{H_2} + \tilde{\mu}_{H_2}(T,p^0) + RTln\left(\frac{p_{H_2}}{p^0}\right)\right] \qquad \text{(S3)}$$

$E^{mol}_{PH_3}$ and $E^{mol}_{H_2}$ are the DFT total energies of the PH_3 and H_2 molecules, including zero-point vibrations. $\tilde{\mu}_{PH_3}(T,p^0)$ and $\tilde{\mu}_{H_2}(T,p^0)$ are the changes of the chemical potentials at different temperatures, which are obtained from thermodynamic tables.[1] p_{PH_3} and p_{H_2} are the partial pressures of PH_3 and H_2. Thus, $\mu_P(T,p)$ is a function of temperature and partial pressures of the PH_3/H_2 gas mixture, which can be directly related to the experimental conditions.

The permitted $\mu_P(T,p)$ range is evaluated into two limits, P-poor and P-rich environments. The P-poor environment limit is defined as the point at which the bulk Ni_2P reduces into metal Ni and PH_3 in the presence of H_2:

$$Ni_2P(bulk) + {}^3\!/_2H_2 \rightarrow 2Ni(bulk) + PH_3 \qquad \text{(S4)}$$

The P-rich environment limit is set at the point beyond which the phosphorus starts to deposit:

$$PH_3 \rightarrow P(bulk) + {}^3\!/_2H_2 \qquad \text{(S5)}$$

Thus, the appropriate variation range for $\mu_P(T,p)$ is

$$E^{bulk}_{Ni_2P} - 2E^{bulk}_{Ni} \le \mu_P(T,p) \le E^{bulk}_{P} \qquad \text{(S6)}$$

where, $E^{bulk}_{Ni_2P}$, E^{bulk}_{Ni} and E^{bulk}_{P} are the DFT total energies of bulk Ni_2P, metal Ni and white phosphorus, respectively.

On the other hand, the chemical potential of sulfur, $\mu_S(T,p)$, is determined by the chemical equilibrium with the gas-phase mixture of H_2 and H_2S,

$$\mu_S(T,p) = \mu_{H_2S}(T,p) - \mu_{H_2}(T,p) \qquad \text{(S7)}$$

where $\mu_{H_2S}(T,p)$ and $\mu_{H_2}(T,p)$ are the chemical potentials of H_2S and H_2, respectively, also evaluated assuming ideal gas behavior. Therefore, $\mu_S(T,p)$ is given by

$$\mu_S(T,p) = \left[\Delta E^{mol} + \Delta\tilde{\mu}_S(T,p^0) + RTln\left(\frac{p_{H_2S}}{p_{H_2}}\right)\right] \tag{S8}$$

where ΔE^{mol} is the difference between the DFT total energy of the H_2S and H_2 molecules $\left(E^{mol}_{H_2S} - E^{mol}_{H_2}\right)$, including zero-point vibrations. $\Delta\tilde{\mu}_S(T,p^0)$ is the difference between the thermal contributions to the chemical potential $\left[\Delta\tilde{\mu}_S(T,p^0) = \tilde{\mu}_{H_2S}(T,p^0) - \tilde{\mu}_{H_2}(T,p^0)\right]$ and are obtained from thermodynamic tables.[1] p_{H_2S} and p_{H_2} are the partial pressures of H_2S and H_2. Large values of $\frac{p_{H_2S}}{p_{H_2}}$ ratio correspond to sulfur-rich conditions, whereas small values of $\frac{p_{H_2S}}{p_{H_2}}$ ratio relate to strongly reducing conditions, in which H_2 is more abundant than H_2S in the gas phase.

S3. Phosphosulfide overlayer on the (0001) surface

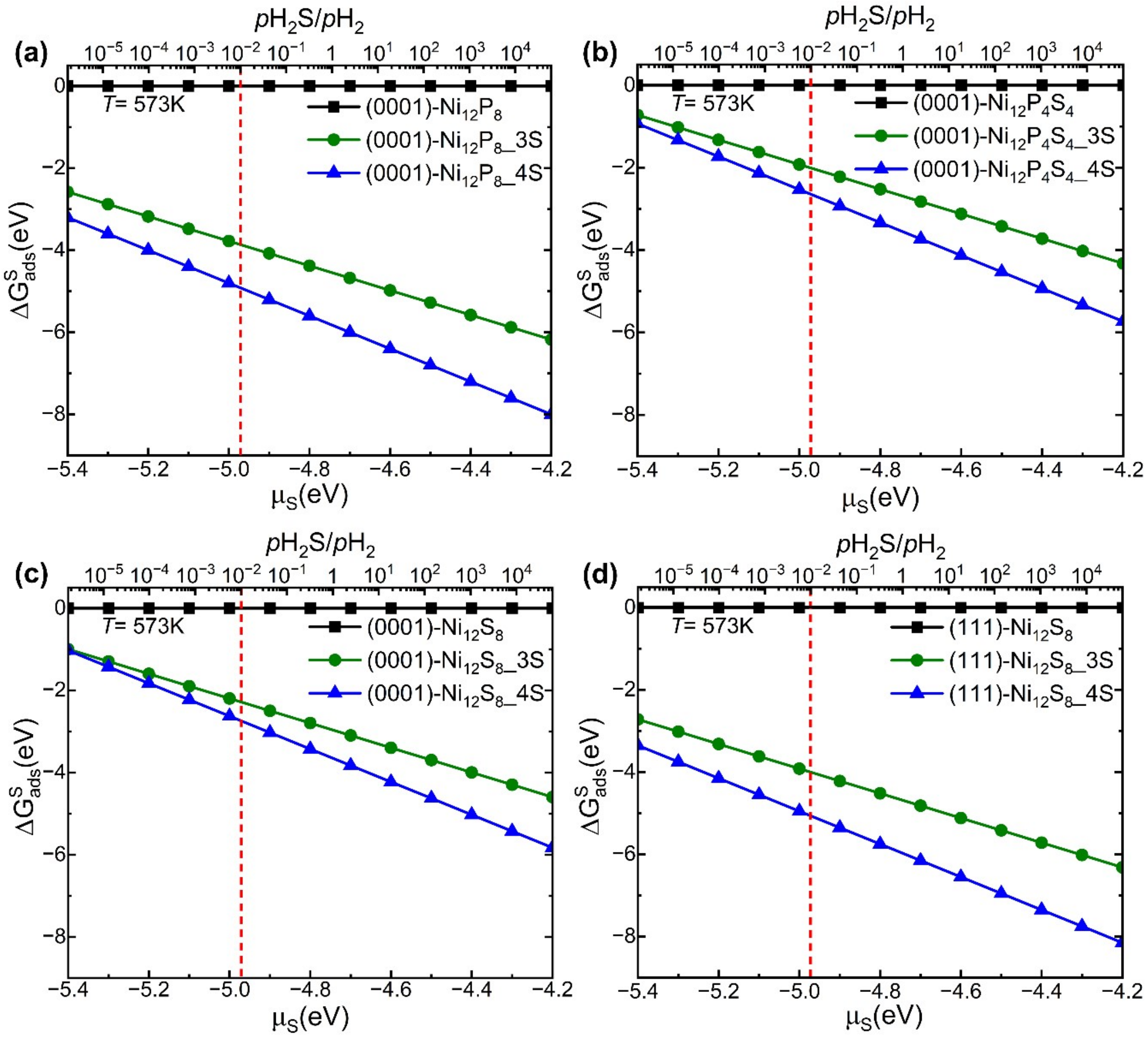

Figure S2. ΔG_{ads}^{S} as a function of $\mu_S(T,p)$ for the (a) (0001)-$Ni_{12}P_8$, (b) (0001)-$Ni_{12}P_4S_4$, (c) (0001)-$Ni_{12}S_8$, and (d) (111)-$Ni_{12}S_8$. The dependence of $\mu_S(T,p)$ with the gas phase H_2S/H_2 mixture is translated into pressure scales for T = 573 K. The red dotted line corresponds to the typical HDS partial pressure ratio, $\frac{p_{H_2S}}{p_{H_2}}$ = 0.01. The clean surface is taken as a reference.

S4. Dissociative adsorption of H_2 onto the phosphosulfide overlayer on the (0001) surface

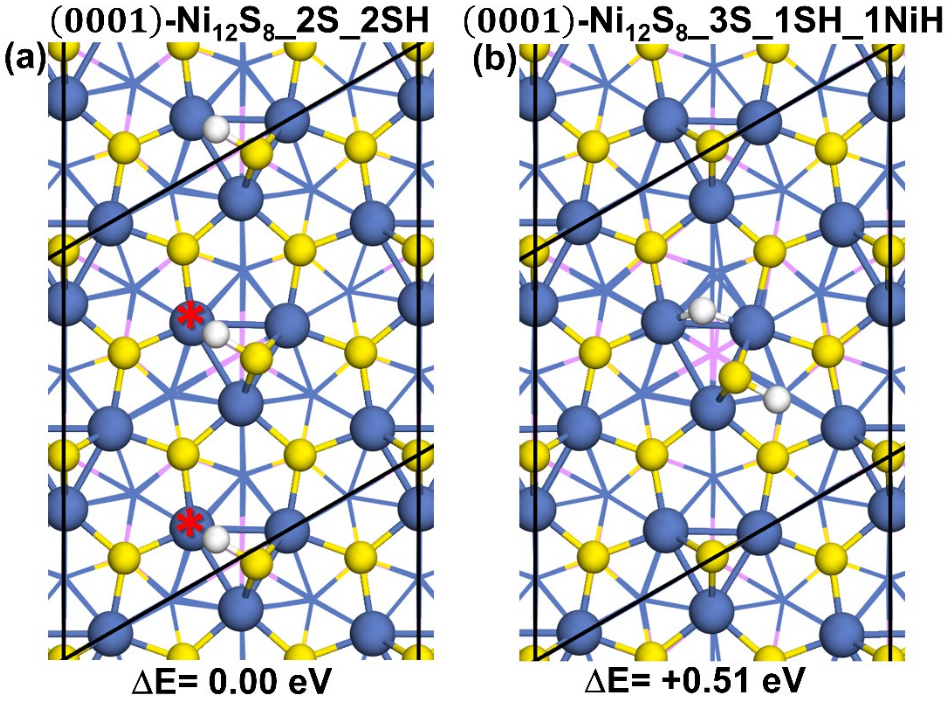

Figure S3. Top view of the optimized structures for the configurations evaluated of the dissociative adsorption of one H_2 molecule on the (0001)-$Ni_{12}S_8$_4S: (a) (0001)-$Ni_{12}S_8$_2S_2SH and (b) (0001)-$Ni_{12}S_8$_3S_1SH_1NiH surfaces. Blue, yellow, and white spheres are the nickel, sulfur, and hydrogen atoms, respectively. Coordinatively unsaturated nickel atoms are marked by a red asterisk.

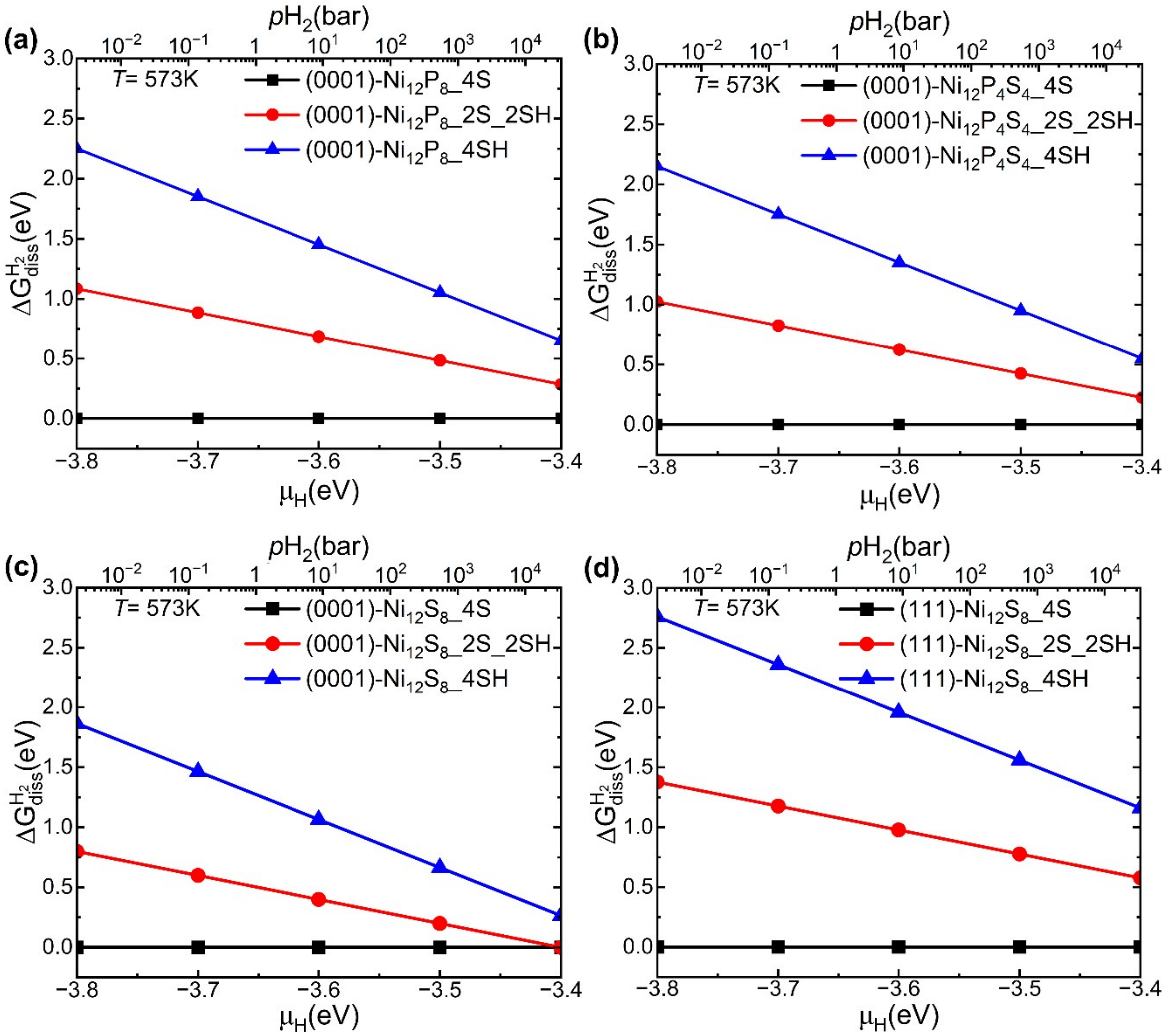
(a)
pH_2(bar)
10^{-2} 10^{-1} 1 10^{1} 10^{2} 10^{3} 10^{4}
T= 573K
(0001)-$Ni_{12}P_8$_4S
(0001)-$Ni_{12}P_8$_2S_2SH
(0001)-$Ni_{12}P_8$_4SH
$\Delta G^{H_2}_{diss}$(eV)
0.0 0.5 1.0 1.5 2.0 2.5 3.0
−3.8 −3.7 −3.6 −3.5 −3.4
μ_H(eV)
(b)
pH_2(bar)
10^{-2} 10^{-1} 1 10^{1} 10^{2} 10^{3} 10^{4}
T= 573K
(0001)-$Ni_{12}P_4S_4$_4S
(0001)-$Ni_{12}P_4S_4$_2S_2SH
(0001)-$Ni_{12}P_4S_4$_4SH
$\Delta G^{H_2}_{diss}$(eV)
0.0 0.5 1.0 1.5 2.0 2.5 3.0
−3.8 −3.7 −3.6 −3.5 −3.4
μ_H(eV)
(c)
pH_2(bar)
10^{-2} 10^{-1} 1 10^{1} 10^{2} 10^{3} 10^{4}
T= 573K
(0001)-$Ni_{12}S_8$_4S
(0001)-$Ni_{12}S_8$_2S_2SH
(0001)-$Ni_{12}S_8$_4SH
$\Delta G^{H_2}_{diss}$(eV)
0.0 0.5 1.0 1.5 2.0 2.5 3.0
−3.8 −3.7 −3.6 −3.5 −3.4
μ_H(eV)
(d)
pH_2(bar)
10^{-2} 10^{-1} 1 10^{1} 10^{2} 10^{3} 10^{4}
T= 573K
(111)-$Ni_{12}S_8$_4S
(111)-$Ni_{12}S_8$_2S_2SH
(111)-$Ni_{12}S_8$_4SH
$\Delta G^{H_2}_{diss}$(eV)
0.0 0.5 1.0 1.5 2.0 2.5 3.0
−3.8 −3.7 −3.6 −3.5 −3.4
μ_H(eV)

Figure S4. $\Delta G^{H_2}_{diss}$ as a function of $\mu_H(T,p)$ for the (a) (0001)-$Ni_{12}P_8$_4S (b) (0001)-$Ni_{12}P_4S_4$_4S, (c) (0001)-$Ni_{12}S_8$_4S, and (d) (111)-$Ni_{12}S_8$_4S surfaces. The dependence of $\mu_H(T,p)$ with the gas phase H_2 is translated into pressure scales for T = 573 K. The nonhydrogenated surface was taken as a reference.

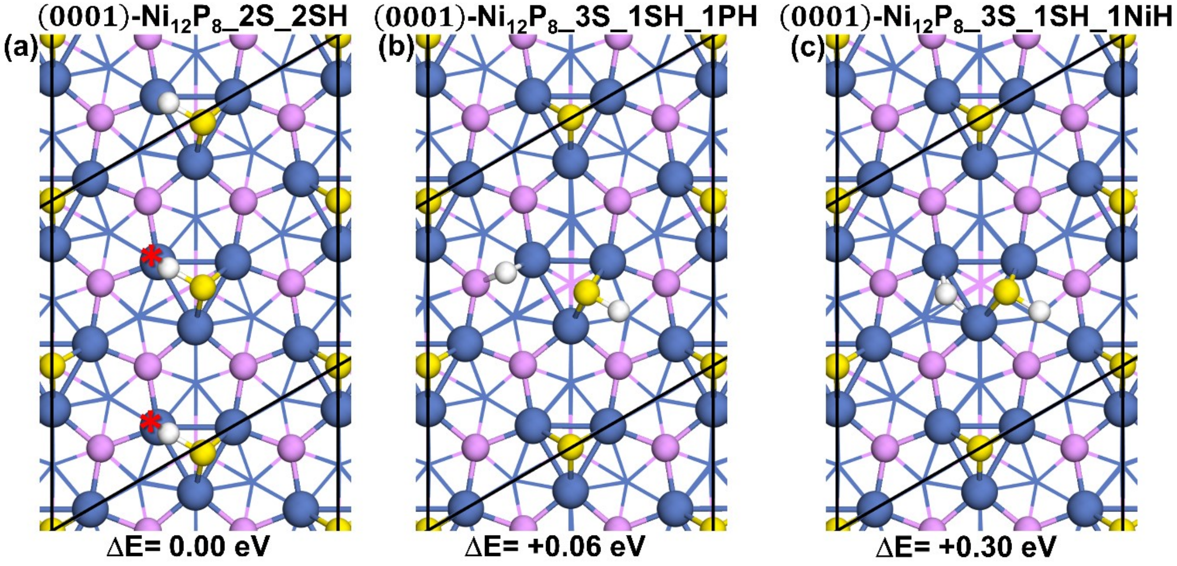

Figure S5. Top view of the optimized structures for the configurations evaluated of the dissociative adsorption of one H_2 molecule on the (0001)-$Ni_{12}P_8$_4S: (a) (0001)-$Ni_{12}P_8$_2S_2SH, (b) (0001)-$Ni_{12}P_8$_3S_1SH_1PH and (0001)-$Ni_{12}P_8$_3S_1SH_1NiH surfaces. Blue, yellow, and white spheres are the nickel, sulfur, and hydrogen atoms, respectively. Coordinatively unsaturated nickel atoms are marked by a red asterisk.

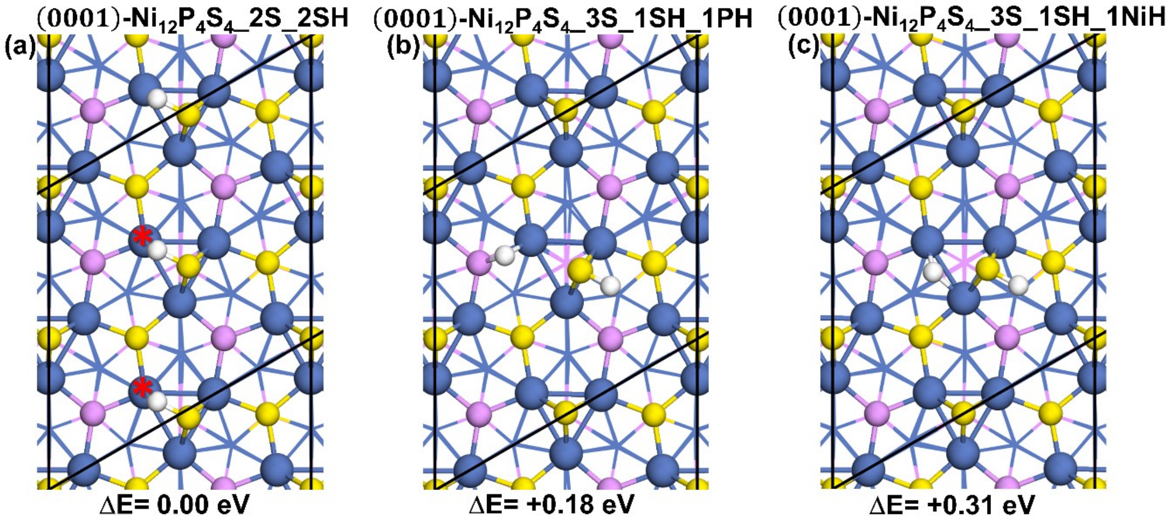

Figure S6. Top view of the optimized structures for the configurations evaluated of the dissociative adsorption of one H_2 molecule on the (0001)-$Ni_{12}P_4S_4$_4S: (a) (0001)-$Ni_{12}P_4S_4$_2S_2SH, (b) (0001)-$Ni_{12}P_4S_4$_3S_1SH_1PH, and (c) (0001)-$Ni_{12}P_4S_4$_3S_1SH_1NiH surfaces. Blue, yellow, and white spheres are the nickel, sulfur, and hydrogen atoms, respectively. Coordinatively unsaturated nickel atoms are marked by a red asterisk.

S5. Dissociative adsorption of H_2 onto the phosphosulfide overlayer on the $(10\bar{1}0)$ surface

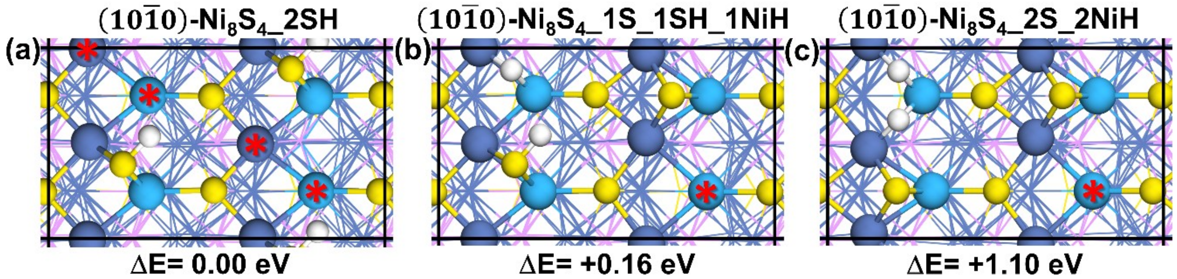

Figure S7. Top view of the optimized structures for the configurations evaluated of the dissociative adsorption of one H_2 molecule on the $(10\bar{1}0)$-Ni_8S_4_2S surface: (a) $(10\bar{1}0)$-Ni_8S_4_2SH, (b) $(10\bar{1}0)$-Ni_8S_4_1S_1SH_1NiH, and (c) $(10\bar{1}0)$-Ni_8S_4_2S_2NiH. Blue, light blue, yellow, and white spheres are the Ni(1) nickel, Ni(2) nickel, sulfur, and hydrogen atoms, respectively. Coordinatively unsaturated Ni(1) and Ni(2) nickel atoms are marked by a red asterisk.

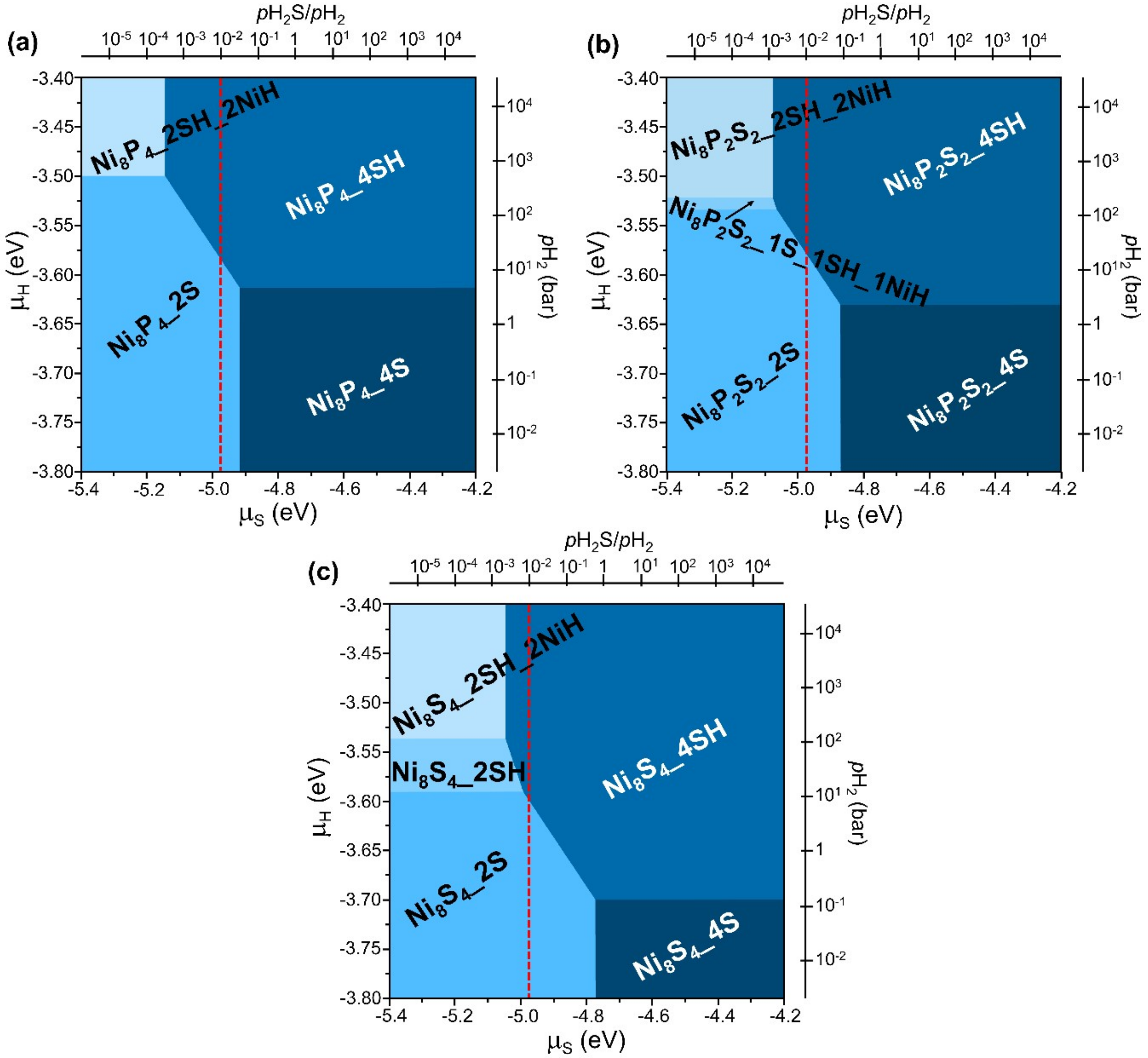

Figure S8. Phase diagrams of the most stable hydrogenated surface composition for the (a) $(10\bar{1}0)$-Ni_8P_4_2S and $(10\bar{1}0)$-Ni_8P_4_4S, (b) $(10\bar{1}0)$-$Ni_8P_2S_2$_2S and $(10\bar{1}0)$-$Ni_8P_2S_2$_4S, and (c) $(10\bar{1}0)$-Ni_8S_4_2S and $(10\bar{1}0)$-Ni_8S_4_4S surfaces as a function of $\mu_H(T,p)$ and $\mu_S(T,p)$. The dependence of the chemical potentials with the gas phase is translated into pressure scales for T = 573 K on the upper x-axis for the H_2S/H_2 mixture and on the right y-axis for H_2. The red dotted line corresponds to the typical HDS partial pressure ratio, $\frac{p_{H_2S}}{p_{H_2}} = 0.01$.

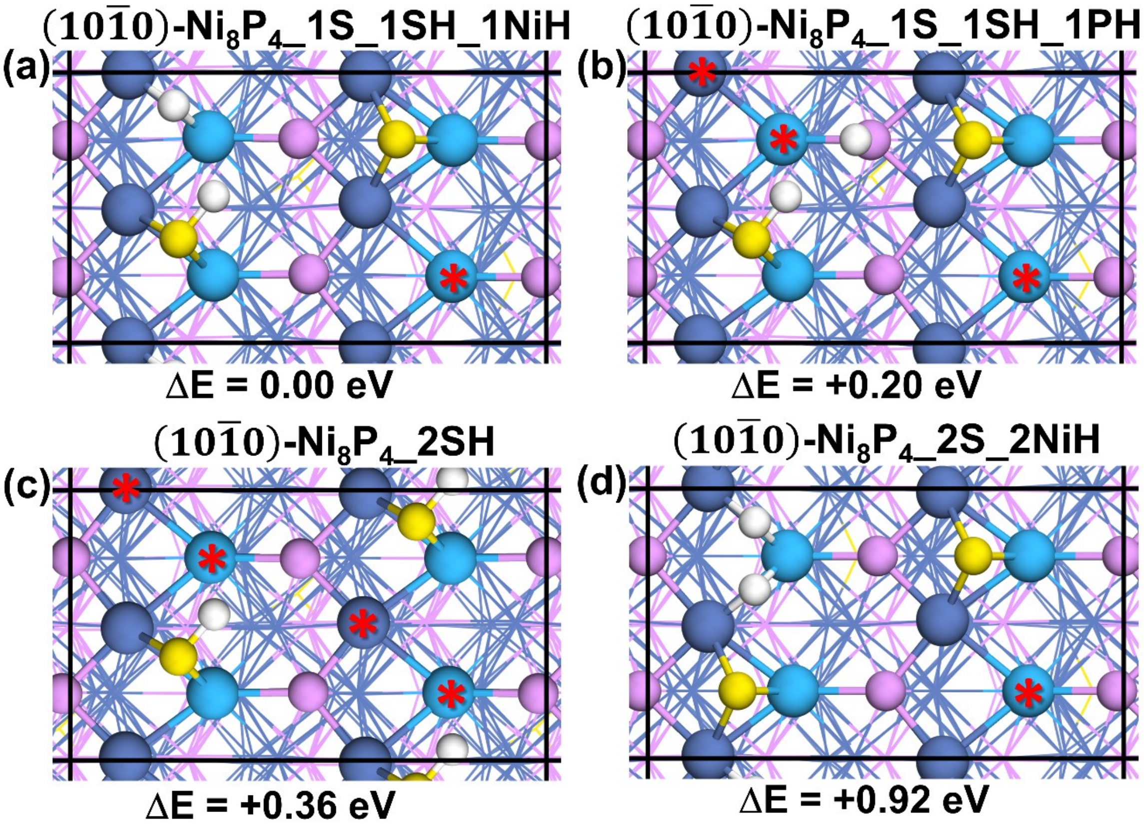

Figure S9. Top view of the optimized structures for the configurations evaluated of the dissociative adsorption of one H_2 molecule on the $(10\bar{1}0)$-Ni_8P_4_2S surface: (a) $(10\bar{1}0)$-Ni_8P_4_1S_1SH_1NiH, (b) $(10\bar{1}0)$-Ni_8P_4_1S_1SH_1PH, (c) $(10\bar{1}0)$-Ni_8P_4_2SH, and (d) $(10\bar{1}0)$-Ni_8P_4_2S_2NiH. Blue, light blue, pink, yellow, and white spheres are the Ni(1) nickel, Ni(2) nickel, phosphorus, sulfur, and hydrogen atoms, respectively. Coordinatively unsaturated Ni(1) and Ni(2) nickel atoms are marked by a red asterisk.

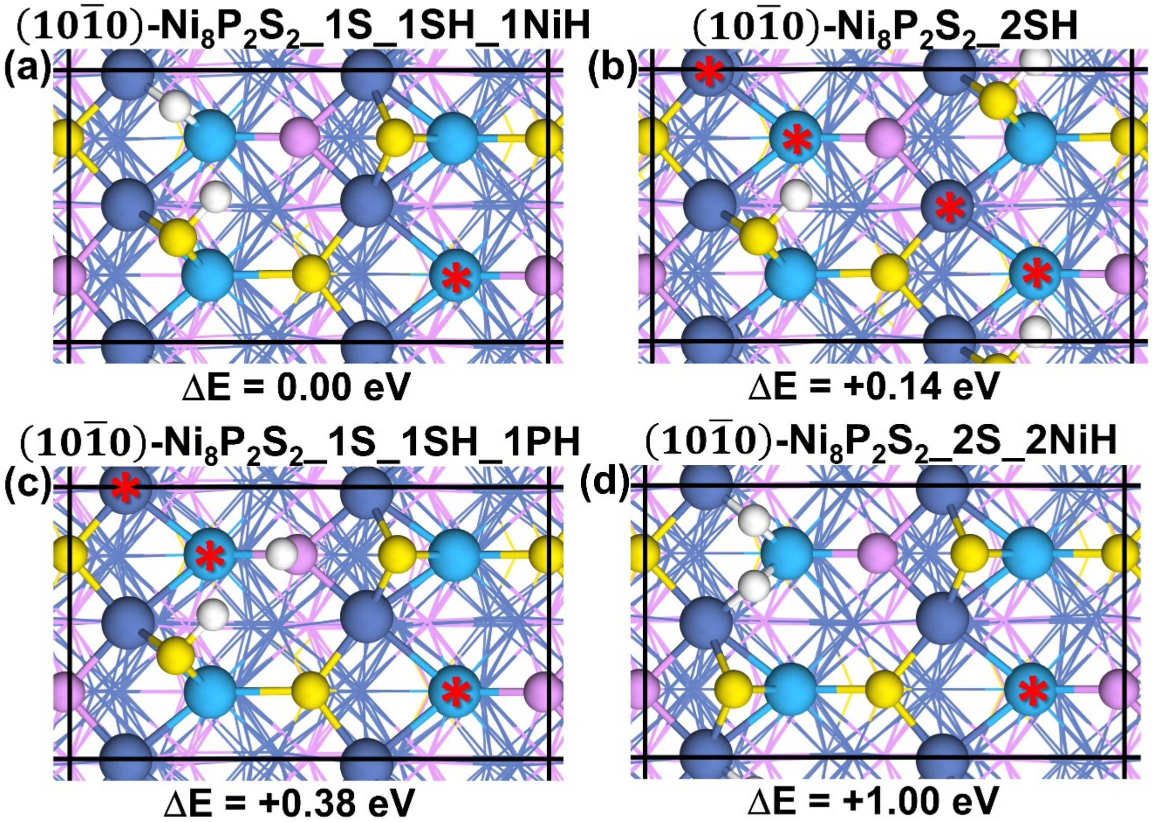

Figure S10. Top view of the optimized structures for the configurations evaluated of the dissociative adsorption of one H_2 molecule on the $(10\bar{1}0)$-$Ni_8P_2S_2$_2S surface: (a) $(10\bar{1}0)$-$Ni_8P_2S_2$_1S_1SH_1NiH, (b) $(10\bar{1}0)$-$Ni_8P_2S_2$_2SH, (c) $(10\bar{1}0)$-$Ni_8P_2S_2$_1S_1SH_1PH, and (d) $(10\bar{1}0)$-$Ni_8P_2S_2$_2S_2NiH. Blue, light blue, pink, yellow, and white spheres are the Ni(1) nickel, Ni(2) nickel, phosphorus, sulfur, and hydrogen atoms, respectively. Coordinatively unsaturated Ni(1) and Ni(2) nickel atoms are marked by a red asterisk.

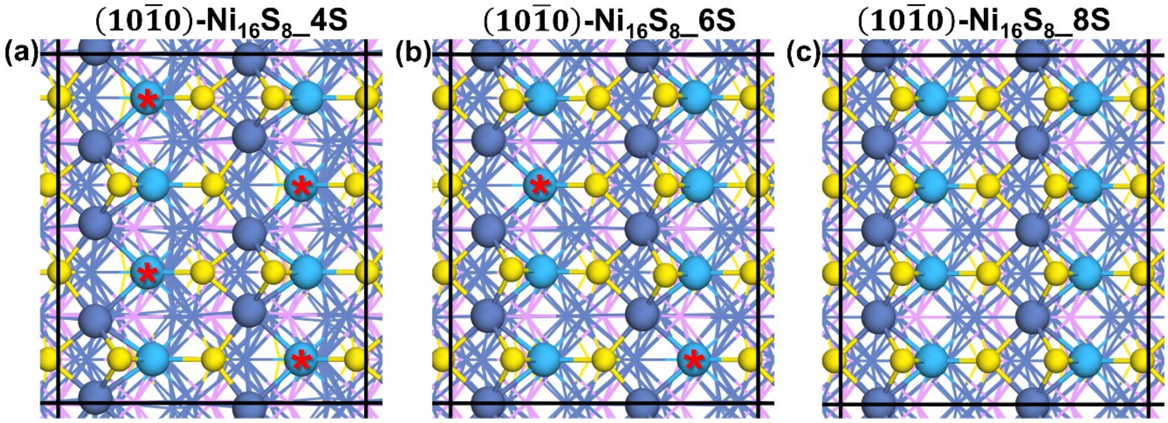

Figure S11. Top view of the optimized structures of the (2x4) supercell: (a) $(10\bar{1}0)$-Ni$_{16}$S$_8$_4S, (b) $(10\bar{1}0)$-Ni$_{16}$S$_8$_6S, and (c) $(10\bar{1}0)$- Ni$_{16}$S$_8$_8S surfaces. Blue, light blue, and yellow spheres are the Ni(1) nickel, Ni(2) nickel, and sulfur atoms, respectively. Coordinatively unsaturated Ni(2) nickel atoms are marked by a red asterisk.

The $(10\bar{1}0)$-Ni$_{16}$S$_8$_4S surface, for instance, is equivalent to the $(10\bar{1}0)$-Ni$_8$S$_4$_2S. Four of the eight T1 sites are covered by S atoms in an alternating pattern, resulting in four coordinatively unsaturated Ni(2) atoms. The $(10\bar{1}0)$-Ni$_{16}$S$_8$_8S surface is equivalent to the $(10\bar{1}0)$-Ni$_8$S$_4$_4S, where all the T1 sites are covered by S atoms. On the other hand, the $(10\bar{1}0)$-Ni$_{16}$S$_8$_6S surface contains two coordinatively unsaturated Ni(2) atoms because six of the eight T1 sites are covered by S atoms.

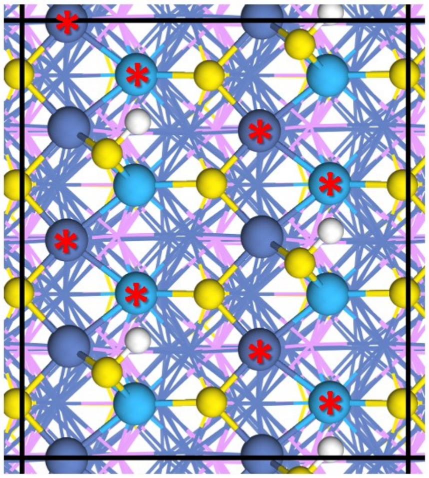

Figure S12. Top view of the optimized structure of the $(10\bar{1}0)$-$Ni_{16}S_8$_4SH surface. Blue, light blue, yellow, and white spheres are the Ni(1) nickel, Ni(2) nickel, sulfur, and hydrogen atoms, respectively. Coordinatively unsaturated Ni(1) and Ni(2) nickel atoms are marked by a red asterisk.

References

1 M. W. Chase Jr., NIST-JANAF Thermochemical Tables, *Phys. Chem. Ref. Data, Monograph 9*, 1998, 1–1951.